Synthesis and physical characterization of nickel oxide nanoparticles and its application study in the removal of ciprofloxacin from contaminated water by adsorption: Equilibrium and kinetic studies

Somayeh Rahdar[a], Abbas Rahdar[b], Chinenye Adaobi Igwegbe[c], Fahimeh Moghaddam[a], Shahin Ahmadi[a],*

[a]*Department of Environmental Health, Zabol University of Medical Sciences, Zabol, Iran, email: rahdar89@gmail.com (S. Radar) nakhzari.f94@gmail.com (F. Moghaddam), Tel. +989184957156, email: sh.ahmadi398@gmail.com (S. Ahmadi)*
[b]*Department of Physics, University of Zabol, Zabol, P. O. Box. 35856-98613, Islamic Iran,*
email: a.rahdarnanophysics@gmail.com (A. Rahdar)
[c]*Department of Chemical Engineering, Nnamdi Azikiwe University, Awka, Nigeria, email: ca.igwegbe@unizik.edu.ng (C.A. Igwegbe)*

ABSTRACT

Considering the risk and importance of antibiotics, especially ciprofloxacin, the allowable discharge level should be reached before disposal to the environment. The aim of this work is to study the application of nickel oxide nanoparticles (NiO NPs) as an efficient adsorbent to remove ciprofloxacin (CIP) from its aqueous solution. Batch experiments were carried out in order to determine the effect of different parameters such as pH of the solution (3–8), contact time (20–120 min), initial CIP concentration (50–200 mg/L) and dosage of NiO NPs (0.04–0.14 g/L) on ciprofloxacin adsorption using NiO NPs. The morphological properties of the NiO NPs were described through the Atomic Force Microscope (AFM), Vibrating Sample Magnetometer (VSM), Dynamic Light Scattering (DLS), X-ray diffraction (XRD) and Fourier transform infrared (FT-IR) techniques. Removal efficiency of 99.8% was obtained at pH of 3, nanoparticle dosage of 0.08 g/L, contact time of 100 min, and initial CIP concentration of 200 mg/L at temperature of 25 ± 2°C. The adsorption experimental data were found to fit best into the pseudo-second-order kinetic model (R^2 = 0.999) than the pseudo-first-order model (R^2 = 0.214) which suggests a chemical adsorption process. The Freundlich adsorption isotherm model best described the removal of ciprofloxacin on NiO NPs (R^2 = 0.988). Maximum adsorption capacity, q_m of 99.81 mg/g was obtained. The adsorption of ciprofloxacin on NiO NPs was found to be favorable since the intensity of adsorption lies within 1 and 10. Based on the results obtained, it could be concluded that the NiO NPs can efficiently remove ciprofloxacin from its aqueous solutions.

Keywords: Drugs removal; Nickel oxide; Antibiotics; Nanoparticles

1. Introduction

Unused therapeutic drugs are sometimes disposed into the sewage system. If these drugs are not degraded or eliminated from the contaminated media, example, through sewage treatment, they will eventually reach the surface and ground waters posing a great threat for drinking water sources [1]. Ciprofloxacin (CIP) classified in fluoroquino-lone class (irresolvable antibiotics [2]) has been widely applied for the treatment of intra-abdominal infections, certain type of infectious diarrhea, respiratory tract infections and urinary tract infections [3] with good results [4]. These antibiotics have a stable naphthol ring which is toxic for microorganisms and makes them persistent in the environment [1].

Several methods were reported for the removal of antibiotics from aqueous environments including nano-filtra-

*Corresponding author.

tion [5], Fenton [6], advanced oxidation methods [7] and electrochemical-assisted photocatalysis [8]. The adsorption method is widely used due to its advantages such as simplicity, low-cost and so on [9,10]. In addition, a recent method for the removal of pollutants in aqueous environments, the heterogeneous photocatalysis using UV-radiation and quantum dots (QDs) is an interesting technique for the treatment of water contaminated with organic materials [11]. A study by Rajabi et al. utilized ZnS QDs, as a pure and doped with Fe^{3+} for photodecolorization of malachite green (MG). The synthesis of QDs was done using the chemical precipitation method in the presence of 2-mercaptoethanol as a capping agent. Maximum removal of malachite green was obtained at 80 mg/L of photocatalyst and pH of 8.0. Results showed that the pure ZnS QDs and Fe^{3+} doped ZnS QDs presented high MG removal efficiency [11]. Another study by Rajabi and Farsi (2015) synthesized pure and transition metal ions (Mn^{2+}, Co^{2+}, Ni^{2+} ions) doped QDs. The photocatalytic activities of the prepared ZnS QDs for the removal of methyl violet were studied. The results demonstrated that doped QDS (for 5% of dopants) effectively decolorized the cationic dye, methyl violet presenting a positive photocatalytic improvement over pure ZnS nanoparticles [12].

Different carbon adsorbers like activated carbon have been used to remove organic and mineral pollutants [13,14]. Recently, some features such as high surface area, and unusual adsorptive properties of metal oxide nanoparticles have attracted the attention of many researchers towards the synthesis of nanoparticles [15]. Nickel oxide (NiO) nanoparticles are very important metallic oxide because of its magnetic and chemical properties [16]. It is believed that the chemical and physical properties of nanoparticles are related to their method of synthesis [17]. The ultrafine nickel oxide particles have found applications in different fields such as film reel production, magnetic elements, ceramics and batteries [17].

So, taking note of these advantages mentioned above, nickel oxide nanometer-sized particles were synthesized using the co-precipitation method. Their structural, magnetic, and morphological properties were characterized via the XRD, VSM, FTIR, and DLS techniques. Finally, the synthesized nickel oxide nanoparticles were characterized as a potential nano-adsorbent in terms of their ability to remove ciprofloxacin from its aqueous solution.

The main purpose of this study is to examine the application of nickel oxide nanoparticles (NiO NPs) as a potential nano-adsorbent for the removal of ciprofloxacin from its aqueous solution. The impact of various factors such as contact time, adsorbent dosage, pH and initial concentration of ciprofloxacin on the adsorptive removal of ciprofloxacin were studied. The adsorption experimental data was also fitted into the adsorption isotherm and kinetic models.

2. Materials and methods

2.1. Materials

Ciprofloxacin (purity > 99.6% and molecular formula: $C_{17}H_{18}FN_3O_3HClH_2O$) was supplied by Sigma-Aldrich, USA. All reagents were of analytical grade and purchased

from Merck (Germany).They were used as purchased without any further purification.

2.2. Preparation of nickel oxide nanoparticles

The NiO NPs were prepared by the co-precipitation method using a previously described method [18]. Then NiO NPs was calcined (annealed) at 700°C.

2.3. Characterization of NiO nanometer-sized particles

Atomic Force Microscope, AFM(A/S DK-2730 (Denmark)) was used to determine themorphological property of the nickel oxide nanoparticles. The AFM characterization was carried out at room temperature in a non-contact mode. The magnetic behavior of the NiO NPs was studied via the vibrating sample magnetometer (VSM) technique (Kavir Precise Magnetic instrument, MDKFT, Iran). The size of nanoparticles was obtained by the dynamic light scattering (DLS) method using a Zetasizer Nano ZS (Malvern Instruments, UK). The X-ray diffraction patterns were taken by means of a Philips diffractometer model PW1800 (The Netherlands) with *CuKα* radiation *(*1.541A⁰). Fourier-transform infrared spectroscopy (FT-IR) was done on a JASCO 640 plus machine (400–4000 cm⁻¹) at room temperature to detect the functional groups present in the NiO NPs taking part in the adsorption of CIP.

2.4. Batch adsorption experiments

The effects of different parameters such as pH (3, 5, 7 and 8), contact time (20, 40, 60, 80, 100 and 120 min), initial CIP concentration (50, 100, 150 and 200 mg/L) and dosage of NiO NPs (0.04, 0.06, 0.08, 0.12 and 0.14 g/L) on the adsorption process were studied. A specified amount of adsorbent was added to Erlenmeyer flasks containing 100 mL of the solutions to be treated having different concentrations of CIP. The pH of the solution was adjusted by adding 0.1 N HCl or 0.1 N NaOH. The flask with its contents was stirred for a specified time at 150 rpm. The resulting solution was centrifuged and the supernatant was analyzed for the residual CIP concentration. The initial and final CIP concentrations in the solutions were determined using a UV–Visible spectrophotometer (Shimadzu Model: CE-1021-UK, Japan) at a wavelength of maximum absorbance (λ_{max}) of 275 nm [2]. The pH was measured using a MIT65 pH meter. The removal efficiency, R (%) was calculated based on the following formula [19,20]:

$$\%R = \frac{(C_0 - C_f)}{C_0} 100 \qquad (1)$$

The amount of CIP adsorbed, q_e (mg/g) was calculated based on the following formula [9,21]:

$$q_e = \frac{(C_0 - C_e)V}{M} \qquad (2)$$

where C_0 and C_e are the initial CIP concentration and equilibrium liquid phase concentration of ciprofloxacin (mg/L) respectively, C_f is the final CIP concentration, V is the volume of the solution (L) and M is the amount of adsorbent, NiO NPs (g).

3. Results and discussion

3.1. Physical results and discussion

The atomic force microscope (AFM) technique for the determination of the properties of a material offers a three dimensional (3D) characterization of nanoparticles with sub-nanometer resolution. In other words, AFM is a useful tool for the analysis of the morphology and size of the nanoparticles [22]. Fig. 1 shows that the NiO NPs are spherical in shape. Large porosity can also be seen implying the availability of a high number of active adsorption sites on the material for the trapping of the adsorbate (CIP) [23].

Magnetization characterization of the NiO NPs was performed using the vibrating sample magnetometer (VSM) technique (Fig. 2). The VSM curve of the NiO NPs at fields of –10000 to 10000 Oe at room temperature is shown in Fig. 2 which confirms the paramagnetic property of the NiO NPs. A magnetic adsorbent is easily removed from the water [24]. It was observed that the NiO NPs produced a higher value of saturation magnetization (0.8 emu/g) with the smallest particle size. It is important to note that particles in nanoscale size have super paramagnetic property [25]. Therefore, the result confirms the formation of NiO particles in the nanometer size range.

Fig. 3 shows the size of NiO nano-adsorbents (a) before and (b) after adsorption by the dynamic light scattering (DLS, Nano-zeta-sizer) at RT. Fig. 3 indicates that the size of the nanoparticles increased after adsorption. It is important to note that the DLS is a useful technique for obtaining the hydrodynamic size of nanoparticles based on their Brownian motion within a nanometer-scale colloidal solution [26–28]. It is also a useful technique for obtaining the size of nanoparticles based on the scattered light by the particles within a colloidal solution. To obtain the nanoparticle size by the DLS technique, the field autocorrelation function of scattered light from nanoparticles as a function of time, $g^1(q,\tau)$ for a given delay time, τ is given by the equation [29,30]:

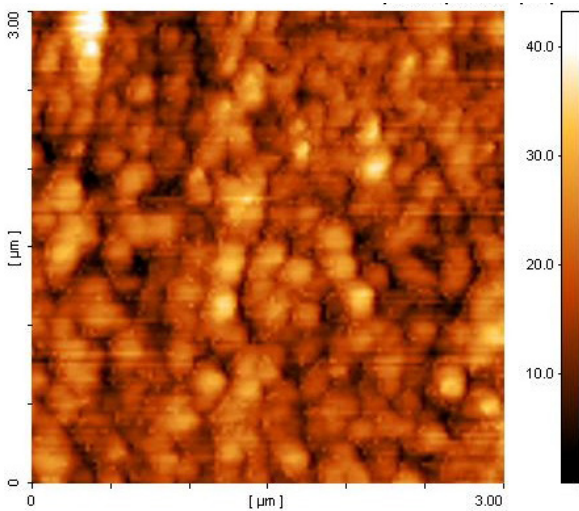$$g^1(q,\tau) = \frac{\langle E(q,t)E^*(q,t+\tau)\rangle}{\langle I(q,t)\rangle} \quad (3)$$

where E^* is the complex conjugate of E and $I(q,\tau)$ is the fluctuating scattered intensity.

Experimentally, the intensity autocorrelation function, $g^2(q,\tau)$ is determined as follows [26–30]:

$$g^2(q,\tau) = \frac{\langle E(q,t)E^*(q,t)E(q,t+\tau)E^*(q,t+\tau)\rangle}{\langle I^2(q,t)\rangle} \quad (4)$$

The normalized autocorrelation function, $g^2(q,\tau)$, is converted to the autocorrelation function of the scattered electrical field, $g^1(q,\tau)$ by the Siegret relationship [26].
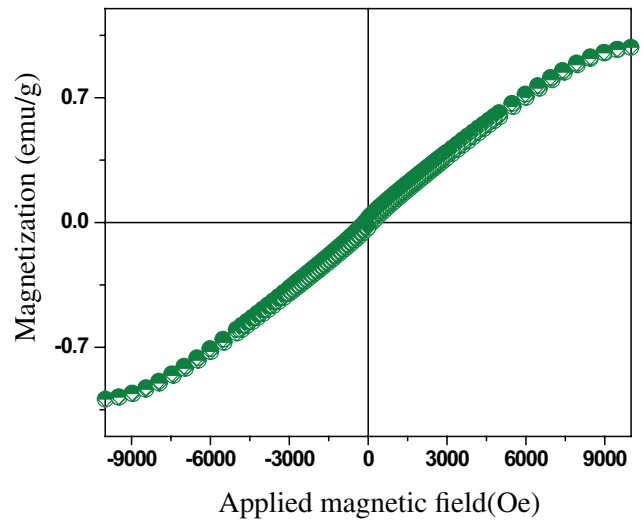

Fig. 2. Magnetization curve for the NiO NPs.
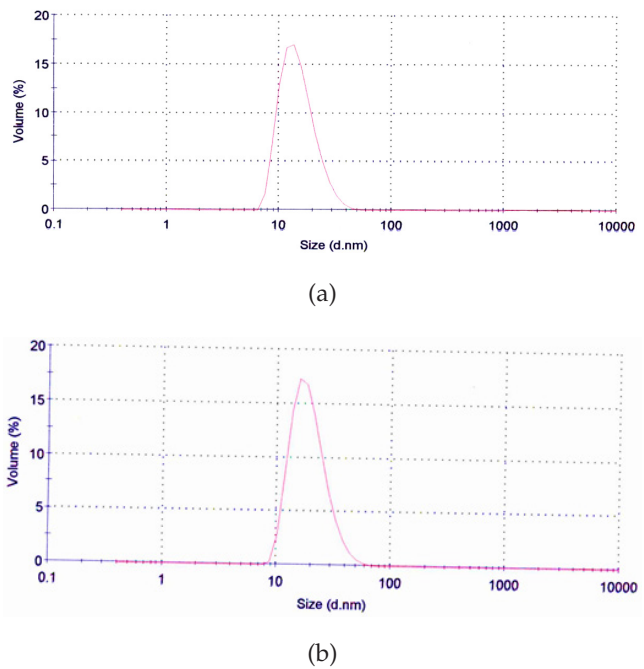

Fig. 1. AFM image of the NiO NPs.

(a)

(b)

Fig. 3. The size distribution of the NiO NPs (a) before and (b) after adsorption at RT.

$$g^2(q,\tau) = 1 + |A \exp(-\Gamma\tau)|^2 \qquad (5)$$

where A is an instrumental constant and Γ is the decay rate.

For a colloidal system containing monodisperse micelles, the function, $g^1(q, \tau)$ is represented by a single exponential decay equation [18,26–29]:

$$g^1(q,\tau) = A \exp(-\Gamma\tau) \qquad (6)$$

In this case, a single exponential function is fitted to the normalized autocorrelation function, $g^1(q,\tau)$ to obtain the decay rate and the size according to the intensity of the scattered light by the nanoparticles in colloidal solution. Scattering intensity of light by nanoparticle is proportional to the 6th power of the particle radius. According to the above-mentioned theory governing the dynamic light scattering (DLS), this tool produces three size distributions including intensity, volume, and number related to the characterization of the nanoparticles. The size distribution by intensity shows how the differently sized particles are detected from a fit to the autocorrelation function of the measured light scattering by DLS. On the other hand, the number and volume distribution are obtained by intensity distribution. The number and volume distribution show the relative proportion of a number of different sized particles, and the volume occupied by the different sized particles.

FTIR tool is a major tool used to identify the functional groups present on the adsorbent. It is also valuable to check the result of loading the adsorbate on the nano-adsorbent surface. The spectral properties of the adsorbent were examined before and after CIP adsorption using the FTIR in the range of 400–4000 cm^{-1} (Fig. 4). It is evident from the data (Fig. 4) that the peak intensities changed after CIP adsorption on the NiO nano-adsorbents surface. The FTIR analysis of the NiO NPs indicates the presence C–Br stretching of alkyl halides (606.74 cm^{-1}), N–H bend of 1° amines (1638.91 cm^{-1}), and C≡N stretch of nitriles (2369.09 cm^{-1}) and O–H stretch, H–bonded of alcohols (3472.27 cm^{-1}). O–H stretch, H–bonded (alcohols, phenols) are very broad and strong band. This band (O–H stretch) took part actively in the adsorptive removal of CIP since the hydrogen bond-
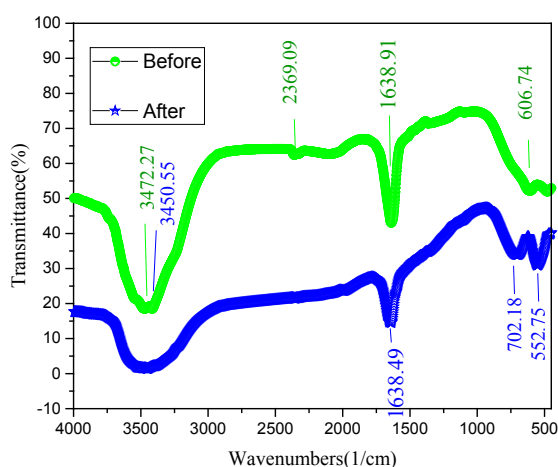
ing plays an active role in adsorption processes [30]. After CIP adsorption, the intensities of the bands were decreased from 606.74, 1638.91 and 3472.27 cm^{-1} to 552.75, 1638.49 and 3450.55 cm^{-1}, respectively. The peak C≡N stretch of nitriles (2369.09 cm^{-1}) disappeared while a new band of C–H stretch bend of alkynes (702.18) was formed. This change in the peaks indicates the interactions of adsorbate with the functional groups of the adsorbent [31].

The XRD pattern of the NiO NPs calcined at 600°C is shown in Fig. 4. The XRD peaks are located at angles (2θ) of 37.40, 43.17 and 62.86 corresponding to (111), (200) and (220) planes of the NiO NPs. The average crystallite size (D) of magnetic nanoparticles was calculated by the Scherer formula ($D_{h,k,l} = 0.9\lambda/\beta_{h,k,l}\cos\theta$, where λ is the wavelength (1.542 Å) (CuKα), β is the full width at half maximum (FWHM) of the line, and θ is the diffraction angle) [32,33]. The average diameter of the adsorbent (D) was calculated to be 24 nm.

3.2. The effect of pH

The parameter, pH directly influences the electrostatic interaction between compounds in the adsorption process [29]. The influence of pH on the removal of CIP and the amount of CIP adsorbed (q_e) on NiO NPs surface are shown in Fig. 6. It is clear from Fig. 6 that the removal percentage of CIP decreased from 97.89% to 91.64% as the pH increased from 3 to 8. Many researchers have reported that the adsorption process is affected by the cationic and anionic forms of the solution due to competition for adsorption among the H$^+$ and OH$^-$ ions with the adsorbate [34]. In this study, the decrease in the removal efficiency of CIP as the pH increased may be attributed to electrostatic repulsion [35] between the positively charged NiO NPs and cationic CIP. The adsorption of CIP was more favorable in the acidic environment due to the presence of H$^+$ on the adsorbent [21]. The increased amount of H$^+$ and reduction of OH$^-$ as well as the increase of positive ion can be the reason for the reduction in efficiency on the absorbent surface [34]. This also due to the competition of CIP with excess OH$^-$ ions for the adsorption sites at lower adsorption pH [36].

3.3. Effect of adsorbent dosage

The effect of NiO Nano-adsorbent dose on the adsorption capacity (q_e) and removal efficiency of CIP was studied by varying the dosages of NiO NPs from 0.04–0.14 g/L (Fig.
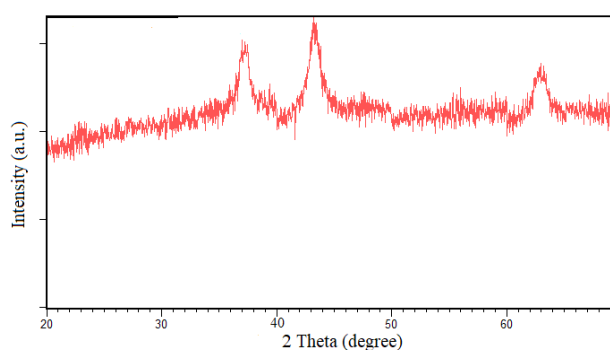

Fig. 4. FTIR spectra of NiO NPs before adsorption and after adsorption.
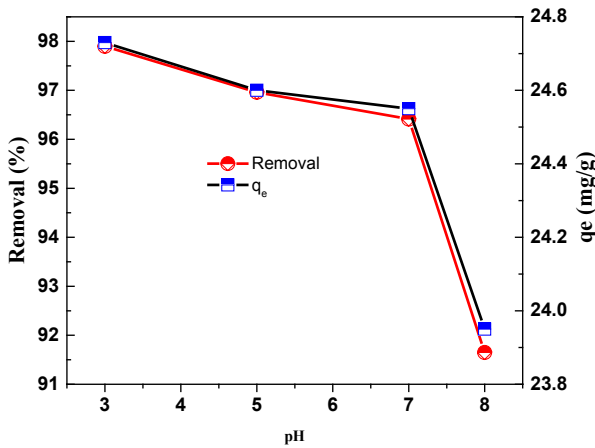

Fig. 5. XRD of NiO NPs calcined at 700°C.

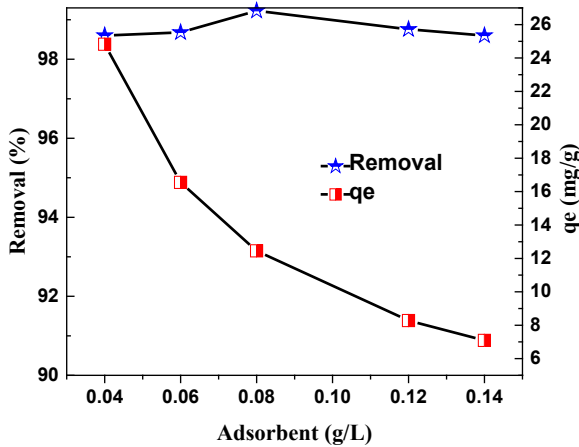Fig. 6. Effect of pH on CIP adsorption on NiO NPs. (C_0 = 100 mg/L, time = 30 min, temp= 25 ± 2°C and NiO NPs dose = 0.04 g/L).

Fig. 7. Effect of adsorbent dose on CIP adsorption on NiO NPs. (C_0 = 100 mg/L, time = 30 min, temp = 25 ± 2°C and pH = 3).

7). The optimum dosage of nano-adsorbent required for CIP adsorption was investigated. It can be seen from Fig. 7 that the adsorption efficiency of CIP increased from 98.6% to 99.22% as the NiO nano-adsorbent dosage increased from 0.04 to 0.08 g/L. The amount of CIP adsorbed on NiO NPs (q_e) at the optimum dosage of 0.08 g/L was 12.45 mg/g. In detail, the level of adsorbate removal significantly depends on the number of active sites and by increasing the dosage of nanoparticles to an appropriate level, whereby the number of available adsorption sites will decrease as a result of decreased adsorption. But beyond dosage of 0.08 g/L, the removal efficiency was decreased which may be due to the fact that the total surface area available for the adsorption of MB reduces as a result of overlapping or aggregation of adsorption sites as the amount of adsorbent dosage is increased [37,38].

3.4. Effect of contact time

Effect of contact time (20, 40, 60, 80, 100 and 120 min) on the removal of CIP at different antibiotic concentrations (50, 100, 150 and 200 mg/L) was studied (Fig. 8). From Fig. 8
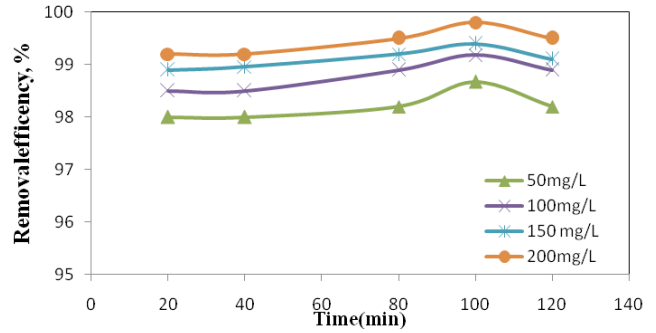

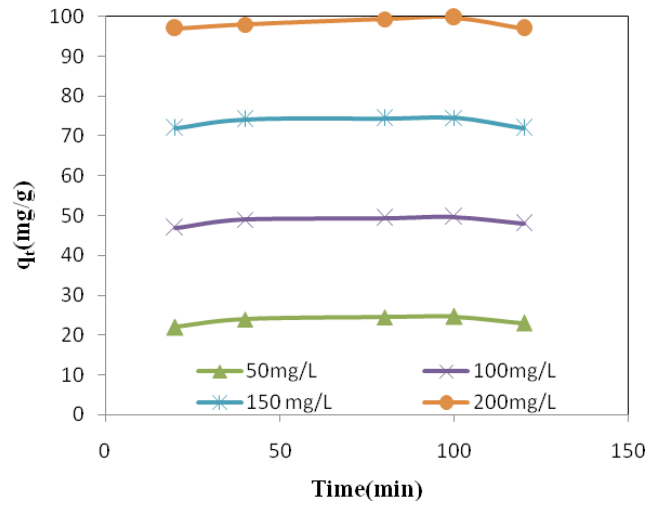Fig. 8. Effect of time on CIP adsorption on NiO NPs. (Dose = 0.04 g/L, Temp = 25 ± 2°C and pH = 3).

Fig. 9. The amount of CIP adsorbed on NiO NPs. (Dose = 0.04 g/L, Temp = 25 ± 2°C and pH = 3).

it can be seen that the removal of CIP increased as contact time increases from 20 to 100 min. Maximum removal of CIP was achieved in the first 100 min (99.8%). The adsorption of CIP in the initial minutes was high, but the adsorption rate decreased (Fig. 9) because of reduced CIP concentration and reduction of the active sites present on the adsorbent surface [39]. The removal efficiency decreased after 100 min because the adsorption sites were occupied [40].

3.5. Adsorption isotherms

Adsorption isotherms are used to determine the relationship between the amount of adsorbate adsorbed and its equilibrium concentration in solution. There are many isotherm models for experimental data analysis and description of equilibrium in adsorption processes such as Langmuir, Freundlich, and Temkin.

The Langmuir isotherm model is presented in Eq. (7) [3,41]:

$$\frac{C_e}{q_e} = \frac{1}{q_m} \cdot \frac{1}{k_L} + \frac{C_e}{q_m} \tag{7}$$

where q_e is the amount of CIP adsorbed (mg/g), q_m is the monolayer adsorption capacity (mg/g), K_L is the Langmuir

isotherm constant related to the affinity of the binding sites and energy of adsorption (L/mg).

The Freundlich isotherm is shown in Eq. (8) [42]:

$$Log q_e = \frac{1}{n} \log C_e + \log k_f \tag{8}$$

where q_e is the amount of CIP adsorbed (mg/g) and C_e is the equilibrium concentration of CIP in solution (mg/L). K_f and n are constants incorporating the factors affecting the adsorption capacity and intensity of adsorption, respectively. The constants, K_f and n were determined from the intercept and slope of the plot of Log q_e versus log C_e (Fig. 10), respectively.

The Tempkin isotherm has been expressed as Eq. (9) [3,43]:

$$q_e = B_1 Ln(A_T) + B_1 Ln(C_e) \tag{9}$$

A plot of q_e vs. Ln C_e enables the constants A_T and B_1 to be determined. B_1 corresponds to the heat of sorption and A is the equilibrium binding constant.

The calculated parameters for the isotherm and kinetic models are presented in Table 1. The correlation coefficient
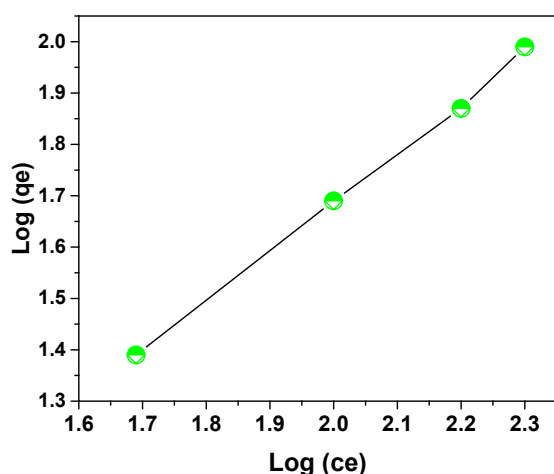
(R^2) was used to determine the kinetic and isotherm model that best fits the CIP adsorption process. The Freundlich isotherm conformed best to the equilibrium data (R^2 of 0.988) than the other models. Also, the intensity of adsorption, n (7.69) lies within the range of 1–10 ($1 < n < 10$) which suggests that the adsorption of CIP on NiO NPs is favorable [44]. The calculated monolayer adsorption capacity, q_m was 99.81 mg/g. Research data of Dhiman and Sharma (2018) fitted best into the Freundlich isotherm than the Langmuir and Temkin models [36].

3.6. Adsorption kinetics

The pseudo-second-order, pseudo-first-order and intraparticle diffusion models were applied in this study to examine the mechanism behind the adsorption of CIP on NiO NPs at pH 3, NiO NPs dosage of 0.08 g/L, and CIP concentration of 100 mg/L at temperature of 25 ± 2°C. The pseudo-first-order rate equation is defined as Eq. (10) [45,46]:

$$\log(q_e - q_t) = \log(q_e) - \frac{k_1}{2.303} t \tag{10}$$

where q_t and q_e are the amounts of CIP adsorbed at time t and at equilibrium (mg/g) and k_1 is the pseudo-first-order rate constant for the adsorption process (min^{-1}).

The pseudo-second-order model can be represented as Eq. (11) [47]:

$$\frac{t}{q_t} = \frac{1}{k_2 q^2} + \frac{t}{q e} \tag{11}$$

where K_2 is the pseudo-second-order rate constant (g mg^{-1} min^{-1}), q_e and q_t are the amounts of CIP adsorbed on the NiO NPs (mg/g) at equilibrium and at time t, respectively.

The intraparticle diffusion plot is generally used to identify the mechanism involved in an adsorption process [48]. The intraparticle diffusion model according to Weber Morris is given by Eq. (12) [48,49]:

$$q_t = k_{pi} t^{0.5} + c \tag{12}$$

Fig. 10. Freundlich plot of CIP adsorption on NiO NPs (pH = 3, NiO NPs dosage = 0.08 g/L, contact time = 100 min).

where c is a constant that provides the information about the thickness of the boundary layer, k_{pi} is the intraparticle

Table 1
Calculated isotherm and kinetic parameters for the adsorption of CIP onto NiO NPs at pH 3 and dosage of 0.08 g/L

Isotherm model			Kinetic model		
Langmuir	q_m (mg/g)	99.81	Pseudo-first-order	q_e (mg/g)	2.79
	K_L (L/mg)	0.018		K_1 (/min)	0.003
	R^2	0.884		R^2	0.214
Freundlich	K_f (mg/g)	131	Pseudo-second-order	q_e (mg/g)	833
	n	7.69		K_2 (g/mg/min)	0.001
	R^2	0.988		R^2	0.999
Temkin	A (L/g)	3.6	Intraparticle diffusion	c	0.3709
	B (J/mol)	128.15		k_{pi} (mg/g min$^{1/2}$)	0.1036
	R^2	0. 8127		R^2	0.9824

diffusion rate constant (mg/g min$^{1/2}$), and q_t is the amount of ciprofloxacin adsorbed (mg/g) at time t (min.).

The pseudo-second-order kinetic showed the best correlation coefficient (R^2 = 0.999) suggesting that the rate-limiting step is chemisorption [50]. Fig. 11 shows the pseudo-second-order kinetic plot for CIP adsorption on NiO NPs. A straight line plot of q_t vs. $t^{0.5}$ was obtained but did not pass through the origin which shows that intraparticle diffusion occurred but is not the rate-determining step [36].

3.7. Comparison with other adsorbents for ciprofloxacin removal

Table 2 shows the adsorption capacities obtained for the removal of CIP on various adsorbents. From the table, it can be seen that the NiO NPs can be used efficiently for the removal of CIP from aqueous environments.

4. Conclusion

The removal for ciprofloxacin (CIP) using nickel oxide nanoparticles (NiO NPs) synthesized by co-precipitation method have been studied. Optimal conditions obtained for the maximum removal of CIP on NiO NPs include initial
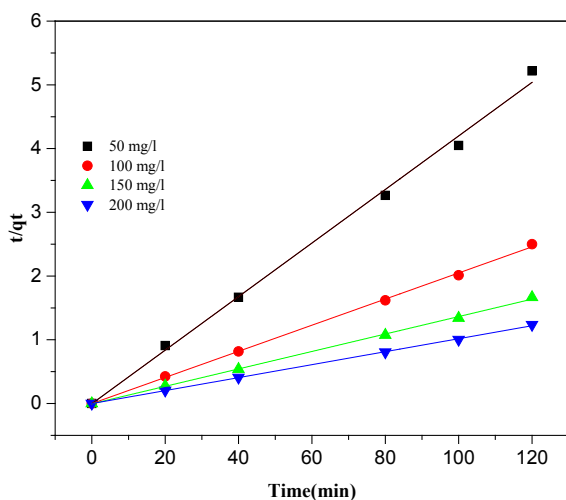

Fig. 11. Pseudo-second-order plot of CIP adsorptionon NiO NPs (pH = 3, NiO NPs dosage = 0.08 g/L, initial CIP concentration = 100 mg/L).

ciprofloxacin concentration of 200 mg/L, pH of 3, NiO NPs dosage of 0.08 g/L and the contact time of 100 min which resulted in 99.81% CIP removal efficiency. The adsorption of CIP on NiO NPs followed the Temkin adsorption isotherm and pseudo-second-order adsorption kinetic more than the other models. The adsorption process was found to be a chemical adsorption process. The results suggest that the NiO NPs can be a potential adsorbent for treating wastewaters contaminated with ciprofloxacin.

Conflicts of Interest

The authors declare that there are no conflicts of interest regarding the publication of this manuscript.

Acknowledgments

References

[1] J.L.Martinez, Environmental pollution by antibiotics and by antibiotic resistance determinants, Environ. Pollut., 157 (2009) 2893–2902.

[2] S. Ahmadi, A. Banach, F.K. Mostafapour, D. Balarak, Study survey of cupric oxide nano particles in removal efficiency of ciprofloxacin antibiotic from aqueous solution: adsorption isotherm study, Desal. Water Treat., 89 (2017) 297–303.

[3] N. Khoshnamvand, S. Ahmadi, F. Kord Mostafapour, Kinetic and isotherm studies on ciprofloxacin an adsorption using magnesium oxide nano particles, J. Appl. Pharm. Sci., 7 (2017) 079–083.

[4] Sh. Ahmadi, F. Kord Mostafapour, Survey of efficiency of dissolved air flotation in removal penicillin G potassium from aqueous solutions, Br. J. Pharm. Res., 15 (2017) 1–11.

[5] J. Wang, Y. Wei, Y. Cheng, Advanced treatment of antibiotic wastewater by nanofiltration: membrane selection and operation optimization, Desal. Water Treat., 52 (2014) 7575–7585.

[6] L.J. Sweetman, L.J. Alcock, J.D. McArthur, E.M. Stewart, G. Triani, S.F. Ralph, Bacterial filtration using carbon nanotube/antibiotic buckypaper membranes, J. Nanomaterials, 2013 (2013) 1–11.

[7] K.J. Choi, S.G. Kim, S.H. Kim, Removal of antibiotics by coagulation and granular activated carbon filtration, J. Hazard. Mater., 151 (2008) 38–43.

[8] A.C. Affam, M. Chaudhuri, Optimization of Fenton treatment of amoxicillin and cloxacillin antibiotic aqueous solution, Desal. Water Treat., 52 (2014) 1878–1884.

Table 2
Adsorption capacities of different adsorbents for CIP removal

Adsorbent	Maximum adsorption capacity, q_m (mg/g) (maximum % removal)	Conditions	Reference
Fe$_3$O$_4$/C	90.1 mg/g (98%)	C_0 = 10 mg/L, dose = 0.02 g, t = 3 h, pH = 7	[40]
ZnO NPs	8.07 mg/g (85.4%)	C_0 = 100 mg/L, t =150 min, pH = 4, dose = 100 mg	[36]
Groundnut shell powder	8.07 mg/g (79.6%)	T = 150 min, C_0 = 100 mg/L, pH = 4, dose = 100 mg	[36]
MgO NPs	3.46 mg/g (85%)	C_0 = 10 mg/L, dose = 1 g/L, pH = 6, t = 60 min	[3]
CuO NPs	105 mg/g (77%)	C_0 = 10 mg/L, pH = 7, dose = 0.1 g/L, t = 60 min	[2]
NiO NPs	99.81 mg/g (99.8%)	C_0 = 100 mg/L, t = 30 min, pH = 3, dose = 0.08 g/L	This study

[9] C.L. Zhang, G.L. Qiao, F. Zhao, Y. Wang, Thermodynamic and kinetic parameters of ciprofloxacin adsorption onto modified coal fly ash from aqueous solution, J. Molec. Liquid., 163 (2011) 53–56.

[10] Sh. Ahmadi, F. Kord Mostafapour, Adsorptive removal of aniline from aqueous solutions by *Pistacia atlantica*(Baneh) shells: isotherm and kinetic studies, J. Sci. Technol. Environ. Inf., 5 (2017) 327–335.

[11] H.R. Rajabi, O. Khani, M. Shamsipur, V. Vatanpour, High-performance pure and Fe³⁺ ion doped ZnS quantum dots as green nanophotocatalysts for the removal of malachite green under UV-light irradiation, J. Hazard. Mater., 250–251 (2013) 370–378.

[12] H.R. Rajabi, M. Farsi, Effect of transition metal ion doping on the photocatalytic activity of ZnS quantum dots: Synthesis, characterization, and application for dye decolorization, J. Mol. Catal. A: Chem., 399 (2015) 53–61.

[13] Sh. Ahmadi, F. Kord Mostafapour, E. Bazrafshan, Removal of aniline and from aqueous solutions by coagulation/flocculation flotation, Chem. Sci. Int. J., 18 (2017) 1–10.

[14] M. Tajbakhsh, M. Farhang, A. Hosseini, MgO nano particles as an efficient and reusable catalyst for aza-Michael reaction, J. Iran. Chem. Soc., 11 (2014) 665–672.

[15] Z. Song, L. Chen, J. Hu, R. Richards, NiO (III) nanosheets as efficient and recyclable adsorbents for dye pollutant removal from wastewater, Nanotechnol., 20 (2009) 275707.

[16] P.A. Sheena, K.P. Priyanka, N.A. Sabu, S. Ganesh, T. Varghese, Effect of electron beam irradiation on the structure and optical properties of nickel oxide nanotubes, Bull. Mater. Sci., 38 (2015) 825–830.

[17] T.L. Lai, W.F. Wang, Y.Y. Shu, Y.T. Liu, C.B. Wang, Evaluation of microwave-enhanced catalytic degradation of 4-chlorophenol over nickel oxides, J. Mole. Catalysis A: Chem., 273 (2007) 303–309.

[18] A. Rahdar, M. Almasi-Kashi, M. Aliahmad, Effect of chain length of oil on location of dye within AOT nanometer-sized droplet microemulsions at constant water content, J Molec. Liq., 233 (2017) 398–402.

[19] Sh. Ahmadi, E. Bazrafshan, F. KordMostafapoor, Treatment of landfill leachate using a combined coagulation and modify bentonite adsorption processes, J. Sci. Eng. Res., 4 (2017) 58–64.

[20] S. Ahmadi, L. Mohammadi, C.A. Igwegbe, S. Rahdar, A.M. Banach, Application of response surface methodology in the degradation of Reactive Blue 19 using H₂O₂/MgO nanoparticles advanced oxidation process, Inter. J. Indust. Chem., 9 (2018) 1–13.

[21] S. Ahmadi, C.A. Igwegbe, Adsorptive removal of phenol and aniline by modified bentonite: adsorption isotherm and kinetics study, Appl. Wat. Sci., 8 (2018) 170.

[22] B. Ruozi, D. Belletti, M.A. Vandelli, F. Pederzoli, P. Veratti, F. Forni, G. Tosi, M. Tonelli, M. Zapparoli, AFM/TEM complementary structural analysis of surface-functionalized nanoparticles, J. Phys. Chem. Biophys., 4 (2014) 150.

[23] S. Banerjee, M.C. Chattopadhyaya, Adsorption characteristics for the removal of a toxic dye, tartrazine from aqueous solutions by a low cost agricultural by-product, Arab. J. Chem., 10 (2017) S3381–S3393.

[24] Y. Liu, Y. Li, X. Zhao, W. Chi, Q. Huang, C. Yu, Y. Xiang, Effect of magnetite nanoparticles on dye absorption properties of magnetite carbon composites, Bull. Mater. Sci., 40 (2017) 367–373.

[25] D. Guo, G. Xie, J. Luo, Mechanical properties of nanoparticles: basics and applications, J. Phys. D: Appl. Phys., 47 (2013).

[26] A. Rahdar, M. Aliahmad, Y. Azizi, NiO nanoparticles: synthesis and characterization, J. Nanostructures, 2 (2015) 145–151.

[27] A. Rahdar, M. Almasi-Kashi, N. Mohamed, Light scattering and optic studies of Rhodamine B-comprising cylindrical-like AOT reversed micelles, J. Molec. Liq., 223 (2016) 1264–1269.

[28] M. Aliahmad, A. Rahdar, F. Sadeghfar, S. Bagheri, M.R. Hajinezhad, Synthesis and biochemical effects of magnetite nanoparticle by surfactant-free electrochemical method in an aqueous system: the current density effect, Nanomedicine Res. J., 1 (2016) 39–46.

[29] T.S. Maryamdokht, A. Rahdar, M. Aliahmad, F. Sadeghfar, M.R. Hajinezhad, M. Jahantigh, P. Shahbazi, J.F. Trant, The synthesis and characterization of a magnetite nanoparticle with potent antibacterial activity and low mammalian toxicity, J. Molec. Liq., 265 (2018) 96–104.

[30] F. Batool, J. Akbar, S. Iqbal, S. Noreen, S.N.A. Bukhari, Study of isothermal, kinetic, and thermodynamic parameters for adsorption of cadmium: an overview of linear and nonlinear approach and error analysis, Bioinorganic Chem. Appl., Article ID 3463724 (2018).

[31] S. Liang, X. Guo, N. Feng, Q. Tian. Isotherms, kinetics and thermodynamic studies of adsorption of Cu²⁺ from aqueous solutions by Mg²⁺/K⁺ type orange peel adsorbent, J. Hazard. Mater., 174 (2010) 756–762.

[32] T.M. Hakami, A.M. Davarpanah, A. Rahdar, S.D. Barrett, Structural and magnetic study and cytotoxicity evaluation of tetra-metallic nanoparticles of Co₀.₅Ni₀.₅CrₓFe₂₋ₓO₄ prepared by co-precipitation, J. Mole. Struct., 1165 (2018) 344–348.

[33] A. Rahdar, M. Aliahmad, Y. Azizi, Synthesis of Cu doped NiO nanoparticles by chemical method, J. Nanostruct., 4 (2014) 145–152.

[34] Y. Gao, Y. Li, L. Zhang, H. Huang, J. Hu, S.M. Shah, X. Su, Adsorption and removal of tetracycline antibiotics from aqueous solution by graphene oxide, J Colloid. Interface Sci., 368 (2012) 540–546.

[35] S. Rahdar, Sh. Ahmadi, Removal of phenol and aniline from aqueous solutions by using adsorption on to *Pistacia terebinthus*: study of adsorption isotherm and kinetics, J. Health Res. Community, 2 (2016) 35–45.

[36] N. Dhiman, N. Sharma, Batch adsorption studies on the removal of ciprofloxacin hydrochloride from aqueous solution using ZnO nanoparticle and groundnut (*Arachis hypogaea*) seed powder: a comparison, Indian Chemical Engineer, 2018, pp. 1–10.

[37] J.N. Nsami, J.K. Mbadcam, The adsorption efficiency of chemically prepared activated carbon from cola nut shells by ZnCl₂ on methylene blue, J. Chem., (2013) 1–7.

[38] B. Das, N.K. Mondal, Calcareous soil as a new adsorbent to remove lead from aqueous solution: equilibrium, kinetic and thermodynamic study, Univ. J. Environ. Res. Technol., 1 (2011) 515–530.

[39] Sh. Ahmadi, F. Kord Mostafapour, Tea waste as a low cost adsorbent for the removal of COD from landfill leachate: kinetic study, J. Sci. Eng. Res., 4 (2017) 103–108.

[40] H. Mao, S. Wang, J.-Y. Lin, Z. Wang, J. Ren, Modification of a magnetic carbon composite for ciprofloxacin adsorption, J. Environ. Sci., 49 (2016) 179–188.

[41] Sh. Ahmadi, F. Kord Mostafapoor, Adsorptive removal of Bisphenol A from aqueous solutions by *Pistacia atlantica*: isotherm and kinetic studies, Pharm. Chem. J., 4 (2017) 1–8.

[42] R. Sarvani, E. Damani, S. Ahmadi, Adsorption isotherm and kinetics study: removal of phenol using adsorption onto modified *Pistaciamutica* shells, Iran J. Health Sci., 6 (2018) 33–42.

[43] A. Sivakumar, Removal of lead and cadmium ions from water using *Annona squamosa* shell: kinetic and equilibrium studies, Desal. Water Treat., 51 (2013) 7700–7709.

[44] M.C. Menkiti, A.O. Okoani, M.I. Ejimofor, Adsorptive study of coagulation treatment of paint wastewater using novel *Brachystegiaeurycoma* extract, Appl. Water Sci., 8 (2018) 189.

[45] D. Balarak, F.K. Mostafapour, Batch equilibrium, kinetics, and thermodynamics study of sulfamethoxazole antibiotics onto *Azolla filiculoides* as a novel biosorbent, Br. J. Pharm. Res., 13 (2016) 1–14.

[46] J.W. Lee, S.P. Choi, R. Thiruvenkatachari, W.G. Shim, H. Moon, Evaluation of the performance of adsorption and coagulation processes for the maximum removal of reactive dyes, Dyes Pigm., 69 (2006) 196–203.

[47] S. Liang, X. Guo, N. Feng, Q. Tian, Isotherms, kinetics and thermodynamic studies of adsorption of Cu²⁺ from aqueous solutions by Mg²⁺/K⁺ type orange peel adsorbents, J. Hazard. Mater., 174 (2010) 756–762.

[48] C.A. Igwegbe, O.D. Onukwuli, J.T. Nwabanne, Adsorptive removal of vat yellow 4 on activated *Mucuna pruriens* (velvet bean) seed shells carbon, Asian J. Chem. Sci., 1 (2016) 1–16.

[49] A.A. El-Bindary, M.A. El-Kawi, A.M. Hafez, I.G. Rashed, E.E. Aboelnaga, Removal of reactive blue 19 from aqueous solution using rice straw fly ash, J. Mater. Environ. Sci., 7 (2016) 1023–1036.

[50] C.A. Igwegbe, P.C. Onyechi, O.D. Onukwuli, I.C. Nwokedi 2016b. Adsorptive treatment of textile wastewater using activated carbon produced from Mucuna pruriens seed shells, World J. Eng. Technol., 4 (2016) 21–37.